

Quantized generalized minimum error entropy for kernel recursive least squares adaptive filtering (This work has been submitted to the IEEE for possible publication. Copyright may be transferred without notice, after which this version may no longer be accessible.)

Jiacheng He, Gang Wang, Kun Zhang, Shan Zhong, Bei Peng, Min Li

Abstract—The robustness of the kernel recursive least square (KRLS) algorithm has recently been improved by combining them with more robust information-theoretic learning criteria, such as minimum error entropy (MEE) and generalized MEE (GMEE), which also improves the computational complexity of the KRLS-type algorithms to a certain extent. To reduce the computational load of the KRLS-type algorithms, the quantized GMEE (QGMEE) criterion, in this paper, is combined with the KRLS algorithm, and as a result two kinds of KRLS-type algorithms, called quantized kernel recursive MEE (QKRMEE) and quantized kernel recursive GMEE (QKRGME), are designed. As well, the mean error behavior, mean square error behavior, and computational complexity of the proposed algorithms are investigated. In addition, simulation and real experimental data are utilized to verify the feasibility of the proposed algorithms.

Index Terms—kernel recursive least square, quantized generalized minimum error entropy, quantized kernel recursive generalized minimum error entropy.

I. INTRODUCTION

The use of kernel approaches in different machine learning and signal processing problems, including classification, regression, clustering, and feature selection, has gained some traction. Support vector machines (SVM) [1], [2], kernel regularization networks (KRN) [3], and kernel principal component analysis (KPSA) [4], among others [5], [6], are effective examples of kernel approaches. The major benefit of kernel approaches is their capacity to universally and linearly describe nonlinear functions in Reproducing Kernel Hilbert Space (RKHS) caused by a Mercer kernel.

Kernel affine projection algorithms (KAPAs) [7], kernel least mean square (KLMS) [7], kernel recursive least squares (KRLS) [8], extended kernel recursive least squares (EX-KRLS) [9], and others are examples of typical kernel adaptive filtering (KAF) algorithms. By assigning a new kernel unit for each fresh sample with the input as the center, radial kernel function-based KAF create a linearly increasing radial

basis function (RBF) network. The errors at each sample are correlated with the coefficients corresponding to each center.

The KRLS is particularly well known for its consistent performance in nonlinear systems with the presence of Gaussian noise. Non-Gaussian noise, however, frequently interferes with several actual applications, including underwater communications [10], parameter identification [11], [12], and acoustic echo cancellation [13], [14]. The presence of the non-Gaussian noise makes the performance of the KRLS algorithm based on the mean square error (MSE) criterion significantly worse.

Thus, new adaptation criteria based on information theoretic learning (ITL) [15] are proposed to overcome these challenges. They are able to benefit from a distribution's higher-order statistics. Examples of ITL criteria that are frequently used to improve the learning efficacy of algorithms include the maximum correntropy criterion (MCC) [16], the generalized maximum correntropy criterion (GMCC) [17], [18], and the minimum error entropy (MEE) criterion [19]. Using the aforementioned learning criteria, the KLMS and KRLS algorithms are integrated with the MCC, and the kernel maximum correntropy (KMC) algorithm [12], [20] and the kernel recursive maximum correntropy (KRMC) algorithms [21], [22] are developed respectively. To further improve the performance of the KAF algorithms, the GMCC is combined with KAF algorithms, as a result of which the generalized kernel maximum correntropy (GKMC) [23] and the kernel recursive generalized maximum correntropy (KRGMC) [24] are developed. MEE criterion is considered to have better performance than MCC [25], and the kernel MEE (KMEE) algorithm [26] and kernel recursive MEE (KRME) algorithm [27] are investigated. Due to its smoothness and stringent positive definiteness, the Gaussian kernel function is generally chosen as the kernel function of the original MEE. The Gaussian kernel function, however, may not always be the optimal choice [17]. The introduction of the generalized Gaussian density leads to the development of the generalized minimum error entropy (GMEE) criterion [28]. Furthermore, the kernel recursive GMEE (KRGME) algorithm with better performance is also derived in [28]. Due to double summa-

This paper was produced by the IEEE Publication Technology Group. They are in Piscataway, NJ.

Manuscript received April 19, 2021; revised August 16, 2021.

tion of GMEE criteria, the computational complexity of the information potential (IP), the fundamental GMEE cost in ITL, is quadratic in terms of sample number. The introduction of GMEE improves the performance of the KRLS algorithm while enhancing the computational complexity to some extent, especially for large-scale data sets.

In this study, the quantizer [29] is utilized to reduce the computational complexity of IP of GMEE and MEE criteria. The quantized kernel recursive GMEE (QKRGME) algorithm and the quantized kernel recursive MEE (QKRMEE) are created by combining the QGMEE criterion with the KRLS method, and QKRMEE is a specific variant of the QKRGME algorithm. In addition, several properties of the QGMEE criterion are discussed to further refine the theoretical framework of QGMEE. The mean error behavior and mean square error behavior of the proposed quantized algorithm are presented. Moreover, the performance and computational complexity of the presented quantized methods are compared with KRGME and KRMEE algorithms.

The main contributions of this study are the following.

(1) The properties of the proposed QGMEE criterion are analysed and discussed.

(2) Two quantized kernel recursive least squares algorithms (QKRMEE and QKRGME), with lower computational complexity, are proposed.

(3) The performance of the proposed algorithm is verified using Electroencephalogram (EEG) data.

The remainder of the study is organized as follows. The properties of the QGMEE are shown in Section II. The proposed KRLS algorithms are presented in Section III. Section IV and Section V are performance analyses and simulations, respectively. Finally, Section VI provides the conclusion.

II. THE PROPERTIES OF THE QUANTIZED GENERALIZED ERROR ENTROPY

A. Quantized generalized error entropy

From [28], the definition of the quantized generalized error entropy is

$$H_\mu(e) = \frac{1}{1-\mu} \log V_{\alpha,\beta}^\mu(e), \quad (1)$$

where μ ($\mu \neq 1, \mu > 0$) stands for the entropy order and e for the error between X and Y . A continuous variable IP $V_{\alpha,\beta}^\mu(e)$ can be written as

$$V_{\alpha,\beta}^\mu(\mathbf{X}, \mathbf{Y}) = V_{\alpha,\beta}^\mu(e) = \int p_{\alpha,\beta}^\mu(e) de = \mathbb{E} \left[p_{\alpha,\beta}^{\mu-1}(e) \right], \quad (2)$$

where $\mathbb{E}[\cdot]$ represents the expectation operation, and μ is set to 2 in [28]. $p_{\alpha,\beta}(\cdot)$ denotes the PDF of error e , as well as $p_{\alpha,\beta}(\cdot)$ can be estimated using

$$p_{\alpha,\beta}(e) \approx \hat{p}_{\alpha,\beta}(e) = \frac{1}{L} \sum_{i=1}^L G_{\alpha,\beta}(e - e_i). \quad (3)$$

Only a limited number of error sets $\{e_i\}_{i=1}^L$ may be obtained in actual applications, and L is the length of Parzen window.

Substituting (3) into (2) with $\mu = 2$, and one method for estimating the IP $V_{\alpha,\beta}(\mathbf{X}, \mathbf{Y})$ is

$$\begin{aligned} \hat{V}_{\alpha,\beta}(\mathbf{X}, \mathbf{Y}) &= \hat{V}_{\alpha,\beta}(e) = \\ &= \frac{1}{L} \sum_{i=1}^L \hat{p}_{\alpha,\beta}(e_i) = \frac{1}{L^2} \sum_{i=1}^L \sum_{j=1}^L G_{\alpha,\beta}(e_i - e_j), \end{aligned} \quad (4)$$

with

$$G_{\alpha,\beta}(e) = \frac{\alpha}{2\beta\Gamma(1/\alpha)} \exp\left(-\frac{|e|^\alpha}{\beta^\alpha}\right), \quad (5)$$

where $G_{\alpha,\beta}(\cdot)$ the generalized Gaussian density function [30], α and $\beta > 0$ refer to the shape and scale parameters, $|\cdot|$ is taking the absolute value, and $\Gamma(\cdot)$ stands for the gamma function. Using estimator (4), the quadratic IP may be calculated.

A quantizer $Q(e_i, \gamma) \in C$ [29] (quantization threshold γ is employed to obtain a codebook $C = \{c_1, c_2, \dots, c_H \in \mathbb{R}^1\}$ in order to lessen the computational load on GMEE. The empirical information potential can be simplified to

$$\begin{aligned} \hat{V}_{\alpha,\beta}(e) &= \frac{1}{L} \sum_{i=1}^L \hat{p}_{\alpha,\beta}(e_i) \approx \hat{V}_{\alpha,\beta}^Q(e) \\ &= \frac{1}{L^2} \sum_{i=1}^L \sum_{j=1}^L G_{\alpha,\beta}[e_i - Q[e_j, \gamma]] \\ &= \frac{1}{L^2} \sum_{i=1}^L \sum_{h=1}^H H_h G_{\alpha,\beta}[e_i - c_h] \\ &= \frac{1}{L} \hat{p}_{\alpha,\beta}^Q(e_i), \end{aligned} \quad (6)$$

where H_h is the number of quantized error samples c_h . And, one can get $L = \sum_{h=1}^H H_h$ and $\int \hat{p}_{\alpha,\beta}^Q(e) de = 1$. The adjustable threshold γ controls the number of elements in the codebook and thus the computational effort of the algorithm.

When $\alpha = 2$, the QGMEE criterion translates into QMEE criterion [29] with the following form:

$$\begin{aligned} \hat{V}_\sigma(e) &= \frac{1}{L} \sum_{i=1}^L \hat{p}_\sigma(e_i) \approx \hat{V}_\sigma^Q(e) \\ &= \frac{1}{L^2} \sum_{i=1}^L \sum_{h=1}^H H_h G_\sigma[e_i - c_h], \end{aligned} \quad (7)$$

where $G_\sigma(\cdot)$ is Gaussian function with the form of $G_\sigma(e) = 1/\sqrt{2\pi}\sigma \exp[-(1/2\sigma^2)e^2]$, parameter σ represents the bandwidth.

From another point of view, a quantizer is a clustering algorithm that classifies the set of errors at a certain distance and the distance is the quantization threshold γ . Predictably, the larger the gamma, the fewer the number H of classes the error set is divided into.

B. Properties

Property 1: When $\gamma = 0$, one can obtain that $\hat{V}_{\alpha,\beta}(e) = \hat{V}_{\alpha,\beta}^Q(e)$.

Proof 1: In the case of $\gamma = 0$, the code book is $C = \{e_1, e_2, \dots, e_L\}$. According to (6), one can obtain $\hat{V}_{\alpha,\beta}(e) = \hat{V}_{\alpha,\beta}^Q(e)$.

Property 2: The proposed cost function $\hat{V}_{\alpha,\beta}^Q(\mathbf{e})$ is bounded, which can be expressed specifically as $\hat{V}_{\alpha,\beta}^Q(\mathbf{e}) \leq \alpha/2\beta\Gamma(1/\alpha)$, with equality if and only if $e_1 = e_2 = \dots = e_L$.

Proof 2: From (6) and (5), we can obtain

$$\hat{V}_{\alpha,\beta}^Q(\mathbf{e}) = \frac{1}{L^2} \sum_{i=1}^L \sum_{j=1}^L \frac{\alpha}{2\beta\Gamma(1/\alpha)} \exp\left(-\frac{|e_i - \mathbf{Q}(e_j, \gamma)|}{\beta^\alpha}\right), \quad (8)$$

since $G_{\alpha,\beta}(e) \leq \alpha/2\beta\Gamma(1/\alpha)$ with equality if and only if $e = 0$. Therefore, one can obtain

$$\hat{V}_{\alpha,\beta}^Q(\mathbf{e}) \leq \frac{1}{L^2} \sum_{i=1}^L \sum_{j=1}^L \frac{\alpha}{2\beta\Gamma(1/\alpha)} = \frac{\alpha}{2\beta\Gamma(1/\alpha)}. \quad (9)$$

Property 3: It holds that $\hat{V}_{\alpha,\beta}^Q(\mathbf{e}) = \sum_{h=1}^H a_h \hat{p}(c_h)$, where $a_h = H_h/L$, and one can obtain $\sum_{h=1}^H a_h = 1$.

Proof 3: It can easily be deduced that

$$\begin{aligned} \hat{V}_{\alpha,\beta}^Q(\mathbf{e}) &= \sum_{h=1}^H \frac{H_h}{L} \left(\frac{1}{L} \sum_{i=1}^L G_{\alpha,\beta}(e_i - c_h) \right) \\ &= \sum_{h=1}^H a_h \hat{p}(c_h). \end{aligned} \quad (10)$$

Remark 1: From property 3, one can obtain that quantized IP is the weighted sum of Parzen's PDF estimator, and this weight is determined by the number H_h in class h .

Property 4: The generalized correntropy criterion (GCC) is a special case of the QGMEE criterion.

Proof 4: When γ is large enough so that $H = 1$, we can obtain $\hat{V}_{\alpha,\beta}^Q(\mathbf{e}) = \hat{p}(c_h)$ from (10). When $H = 1$ and $C = \{0\}$, for the more special case, (10) can be further written as

$$\hat{V}_{\alpha,\beta}^Q(\mathbf{e}) = \frac{1}{L} \sum_{i=1}^L G_{\alpha,\beta}(e_i), \quad (11)$$

which is GCC in [17].

Remark 2: The GCC measures the local similarity at zero, while the QGMEE criterion measures the average similarity about every c_h .

Property 5: When scale parameter β is sufficiently big, we can get

$$\begin{aligned} \hat{V}_{\alpha,\beta}^Q(\mathbf{e}) &\approx \\ &\frac{\alpha}{2\beta\Gamma(1/\alpha)} - \frac{\alpha}{2|\beta|^{\alpha+1}\Gamma(1/\alpha)} \sum_{i=1}^L \sum_{h=1}^H \frac{H_h}{L^2} |e_i - c_h|^\alpha, \end{aligned} \quad (12)$$

where $1/L \sum_{i=1}^L |e_i - c_h|^\alpha$ is the α -order moment of error about c_h

Proof 5: By using Taylor series, (6) can be rewritten as

$$\begin{aligned} \hat{V}_{\alpha,\beta}^Q(\mathbf{e}) &= \frac{1}{L^2} \sum_{i=1}^L \sum_{h=1}^H H_h G_{\alpha,\beta}(e_i - c_h) \\ &= \frac{\alpha}{2\beta\Gamma(1/\alpha)L^2} \sum_{i=1}^L \sum_{h=1}^H \sum_{t=0}^{\infty} \frac{1}{t!} H_h \left(-\left| \frac{e_i - c_h}{\beta} \right|^\alpha \right)^t, \end{aligned} \quad (13)$$

and when β is sufficiently big, we can obtain

$$\begin{aligned} \hat{V}_{\alpha,\beta}^Q(\mathbf{e}) &\approx \frac{\alpha}{2\beta\Gamma(1/\alpha)L^2} \sum_{i=1}^L \sum_{h=1}^H H_h \left[1 - \frac{1}{|\beta|^\alpha} |e_i - c_h|^\alpha \right] \\ &= \frac{\alpha}{2\beta\Gamma(1/\alpha)} - \frac{\alpha}{2|\beta|^{\alpha+1}\Gamma(1/\alpha)} \sum_{i=1}^L \sum_{h=1}^H \frac{H_h}{L^2} |e_i - c_h|^\alpha. \end{aligned} \quad (14)$$

Property 6: In the case of regression model $\mathbf{f}(\mathbf{u}) = \mathbf{w}^T \mathbf{u}$ with a vector \mathbf{w} of weights that need to be estimated, and \mathbf{w} the optimal solution based on the QGMEE criterion is $\mathbf{w} = N_{QGMEE}^{-1} M_{QGMEE}$, where $M_{QGMEE} = \sum_{i=1}^L \sum_{h=1}^H H_h \mathbf{G}_{\alpha,\beta}(e_i - c_h) |e_i - c_h|^{\alpha-2} (d_i - c_h) \mathbf{u}_i$ and $N_{QGMEE} = \sum_{i=1}^L \sum_{h=1}^H H_h \mathbf{G}_{\alpha,\beta}(e_i - c_h) |e_i - c_h|^{\alpha-2} \mathbf{u}_i \mathbf{u}_i^T$.

Proof 6: The gradient of the cost function $\hat{V}_{\alpha,\beta}^Q(\mathbf{e})$ with respect to \mathbf{w} can be written as

$$\begin{aligned} &\frac{\partial \hat{V}_{\alpha,\beta}^Q(\mathbf{e})}{\partial \mathbf{w}} \\ &= \frac{1}{L^2} \frac{\alpha}{\beta^\alpha} \sum_{i=1}^L \sum_{h=1}^H \left[H_h \mathbf{G}_{\alpha,\beta}(e_i - c_h) |e_i - c_h|^{\alpha-1} \right] \\ &\quad \times \text{sign}(e_i - c_h) \mathbf{u}_i \\ &= \frac{\alpha}{L^2 \beta^\alpha} \sum_{i=1}^L \sum_{h=1}^H \left[H_h \mathbf{G}_{\alpha,\beta}(e_i - c_h) |e_i - c_h|^{\alpha-2} \right] \\ &\quad \times [(d_i - c_h) - \mathbf{w}_n^T \varphi_i] \mathbf{u}_i \\ &= \frac{\alpha}{L^2 \beta^\alpha} \sum_{i=1}^L \sum_{h=1}^H H_h \mathbf{G}_{\alpha,\beta}(e_i - c_h) |e_i - c_h|^{\alpha-2} (d_i - c_h) \mathbf{u}_i \\ &\quad - \frac{\alpha}{L^2 \beta^\alpha} \sum_{i=1}^L \sum_{h=1}^H H_h \mathbf{G}_{\alpha,\beta}(e_i - c_h) |e_i - c_h|^{\alpha-2} \mathbf{u}_i \mathbf{u}_i^T \mathbf{w}. \\ &= \frac{\alpha}{L^2 \beta^\alpha} M_{QGMEE} - \frac{\alpha}{L^2 \beta^\alpha} N_{QGMEE} \mathbf{w}. \end{aligned} \quad (15)$$

Setting (15) equal to zero, and one can obtain $\mathbf{w} = N_{QGMEE}^{-1} M_{QGMEE}$, which proves the property 6. Property 6 is utilized to deal with regression problem in [28], and the QGMEE adaptive filtering is developed.

III. KERNEL ADAPTIVE FILTERING BASED ON QGMEE

The input vector $\mathbf{u}_n \in \mathbb{U}$ is considered to be transformed into a hypothesis space \mathbb{K} by the nonlinear mapping $\mathbf{f}(\cdot)$. The input space \mathbb{U} is a compact domain of \mathbb{R}^M , and the output $d_n \in \mathbb{R}^1$ can be described from

$$d_n = \mathbf{f}(\mathbf{u}_n) + \mathbf{v}_n, \quad (16)$$

where \mathbf{v}_n denote the zero-mean noise. RKHS with a Mercer kernel $\kappa(\mathbf{X}, \mathbf{Y})$ will be the learning hypotheses space. The norms used in this study are all l_2 -norms. The commonly used Gaussian kernel with bandwidth σ is utilized:

$$\kappa(\mathbf{X}, \mathbf{Y}) = G_\sigma(\mathbf{X} - \mathbf{Y}) = \frac{1}{\sqrt{2\pi}\sigma} \exp\left(-\frac{1}{2\sigma^2} \|\mathbf{X} - \mathbf{Y}\|^2\right). \quad (17)$$

Theoretically, every Mercer kernel will produce a distinct hypothesis feature space [31]. As a result, the input data $\{\mathbf{u}_1, \mathbf{u}_2, \dots, \mathbf{u}_N\}$ will be translated into the feature space as $\{\varphi_1, \varphi_2, \dots, \varphi_N\}$ (N represents the total number of the input

data), rendering it impossible to do a straight calculation. Instead, using the well-known "kernel trick" [31], one can get the inner production from (17):

$$\varphi_i^T \varphi_j = \kappa(\mathbf{u}_i, \mathbf{u}_j) = \frac{1}{\sqrt{2\pi\sigma}} \exp\left(-\frac{1}{2\sigma^2} \|\mathbf{u}_i - \mathbf{u}_j\|^2\right). \quad (18)$$

The filter output can be expressed as $\mathbf{w}_n^T \boldsymbol{\varphi}_n$ for each time point n , where \mathbf{w}_n is a weight vector in the high-dimensional hypothesis space \mathbb{K} , therefore, the output error can be written separately as

$$e_n = d_n - \mathbf{w}_n^T \boldsymbol{\varphi}_n. \quad (19)$$

A. Kernel recursive QGMEE and QMEE algorithm

According to the QGMEE criterion, one can obtain the cost function with the following form:

$$J_{QGMEE}(\mathbf{w}_n) = \frac{1}{L^2} \lambda^{i+h} \sum_{i=1}^L \sum_{h=1}^H H_h G_{\alpha,\beta}(e_i - c_h) - \frac{1}{2} \vartheta_1 \|\mathbf{w}_n\|^2, \quad (20)$$

where $0 < \lambda \leq 1$ stands for the exponential forgetting factor. The gradient of (20) with respect to \mathbf{w}_n is

$$\begin{aligned} \frac{\partial J_{QGMEE}(\mathbf{w}_n)}{\partial \mathbf{w}_n} &= -\vartheta_1 \mathbf{w}_n \\ &+ \frac{\alpha}{L^2 \beta^\alpha} \sum_{i=1}^L \sum_{h=1}^H \left(\lambda^{i+h} H_h G_{\alpha,\beta}(e_i - c_h) |e_i - c_h|^{\alpha-2} \right. \\ &\quad \left. \times [(d_i - c_h) - \mathbf{w}_n^T \boldsymbol{\varphi}_i] \boldsymbol{\varphi}_i \right). \end{aligned} \quad (21)$$

By applying a formal transformation to equation (21), (21) can be further written as

$$\begin{aligned} \frac{\partial J_{QGMEE}(\mathbf{w}_n)}{\partial \mathbf{w}_n} &= \\ \frac{\alpha}{L^2 \beta^\alpha} \boldsymbol{\Phi}_L \boldsymbol{\Lambda}_L \mathbf{d}_L - \frac{\alpha}{L^2 \beta^\alpha} \boldsymbol{\Phi}_L \boldsymbol{\Lambda}_L \boldsymbol{\Phi}_L^T \mathbf{w}_n - \vartheta_1 \mathbf{w}_n, \end{aligned} \quad (22)$$

where

$$\begin{cases} \boldsymbol{\Phi}_L = [\varphi_1 \ \varphi_2 \ \cdots \ \varphi_L] = [\boldsymbol{\Phi}_{L-1} \ \varphi_L], \\ \mathbf{d}_L = [d_1 - c_h \ d_2 - c_h \ \cdots \ d_h - c_h]^T \\ = [\mathbf{d}_{L-1} \ d_h - c_h]^T, \\ \boldsymbol{\Lambda}_L = \begin{bmatrix} \boldsymbol{\Lambda}_{L-1} & \mathbf{0} \\ \mathbf{0} & \theta_L \end{bmatrix}, \\ [\boldsymbol{\Lambda}_L]_{ij} = \begin{cases} \sum_{h=1}^H \lambda^{i+h} H_h G_{\alpha,\beta}(e_i - c_h) |e_i - c_h|^{\alpha-2}, & i = j, \\ 0, & i \neq j, \end{cases} \\ \theta_L = \sum_{h=1}^H \lambda^{L+h} H_h G_{\alpha,\beta}(e_L - c_h) |e_L - c_h|^{\alpha-2}. \end{cases} \quad (23)$$

To solve for the extreme values, the gradient of (21) is set to zero, and one can get

$$\mathbf{w}_n = \left(\boldsymbol{\Phi}_L \boldsymbol{\Lambda}_L \boldsymbol{\Phi}_L^T + \frac{L^2 \beta^\alpha}{\alpha} \vartheta_1 \mathbf{I} \right)^{-1} \boldsymbol{\Phi}_L \boldsymbol{\Lambda}_L \mathbf{d}_L. \quad (24)$$

Utilizing the kernel trick, (24) can be rewritten as

$$\mathbf{w}_n = \boldsymbol{\Phi}_L \left(\boldsymbol{\Phi}_L^T \boldsymbol{\Phi}_L + \beta^\alpha \vartheta_2 \boldsymbol{\Lambda}_L^{-1} \right)^{-1} \mathbf{d}_L \quad (25)$$

with $\vartheta_2 = L^2 \vartheta_1 / \alpha$.

Given that the input and weight \mathbf{w}_n are observed to combine linearly, one can obtain

$$\mathbf{w}_n = \mathbf{A}_L \mathbf{d}_L, \quad (26)$$

where $\mathbf{A}_L = \boldsymbol{\Phi}_L \mathbf{Q}_L$ and $\mathbf{Q}_L = \left(\boldsymbol{\Phi}_L^T \boldsymbol{\Phi}_L + \beta^\alpha \vartheta_2 \boldsymbol{\Lambda}_L^{-1} \right)^{-1}$. Then, we can get the expression for \mathbf{Q}_L^{-1}

$$\begin{aligned} \mathbf{Q}_L^{-1} &= \boldsymbol{\Phi}_L^T \boldsymbol{\Phi}_L + \beta^\alpha \vartheta_2 \boldsymbol{\Lambda}_L^{-1} \\ &= \begin{bmatrix} \boldsymbol{\Phi}_{L-1}^T \\ \varphi_L^T \end{bmatrix} \begin{bmatrix} \boldsymbol{\Phi}_{L-1} & \varphi_L \end{bmatrix} + \beta^\alpha \vartheta_2 \begin{bmatrix} \boldsymbol{\Lambda}_{L-1}^{-1} & 0 \\ 0 & \theta_L^{-1} \end{bmatrix} \\ &= \begin{bmatrix} \mathbf{Q}_{L-1}^{-1} & \mathbf{h}_L \\ \mathbf{h}_L^T & \varphi_L^T \varphi_L + \beta^\alpha \vartheta_2 \theta_L^{-1} \end{bmatrix}, \end{aligned} \quad (27)$$

where $\mathbf{h}_L = \boldsymbol{\Phi}_{L-1}^T \varphi_L$. According to the block matrix inversion, one can obtain that

$$\mathbf{Q}_L = \begin{bmatrix} \mathbf{Q}_{L-1} + \mathbf{z}_L \mathbf{z}_L^T \mathbf{r}_L^{-1} & -\mathbf{z}_L \mathbf{r}_L^{-1} \\ -\mathbf{z}_L^T \mathbf{r}_L^{-1} & \mathbf{r}_L^{-1} \end{bmatrix}, \quad (28)$$

where $\mathbf{z}_L = \mathbf{Q}_{L-1} \mathbf{h}_L = \mathbf{Q}_{L-1} \boldsymbol{\Phi}_{L-1}^T \varphi_L$ and $\mathbf{r}_L = \varphi_L^T \varphi_L + \beta^\alpha \vartheta_2 \theta_L^{-1} - \mathbf{z}_L^T \mathbf{h}_L$. Substituting (24) and (28) into $\mathbf{A}_L = \boldsymbol{\Phi}_L \mathbf{Q}_L$, and we can get

$$\begin{aligned} \mathbf{A}_L &= \begin{bmatrix} \mathbf{Q}_{L-1} + \mathbf{z}_L \mathbf{z}_L^T \mathbf{r}_L^{-1} & -\mathbf{z}_L \mathbf{r}_L^{-1} \\ -\mathbf{z}_L^T \mathbf{r}_L^{-1} & \mathbf{r}_L^{-1} \end{bmatrix} \mathbf{d}_L \\ &= \begin{bmatrix} \mathbf{Q}_{L-1} + \mathbf{z}_L \mathbf{z}_L^T \mathbf{r}_L^{-1} & -\mathbf{z}_L \mathbf{r}_L^{-1} \\ -\mathbf{z}_L^T \mathbf{r}_L^{-1} & \mathbf{r}_L^{-1} \end{bmatrix} \begin{bmatrix} \mathbf{d}_{L-1} \\ d_L - c_h \end{bmatrix} \\ &= \begin{bmatrix} \mathbf{A}_{L-1} - \mathbf{z}_L \mathbf{r}_L^{-1} (d_L - c_h) \\ \mathbf{r}_L^{-1} (d_L - c_h) \end{bmatrix}. \end{aligned} \quad (29)$$

According to the above-detailed derivation, the pseudo-code of the proposed QKGMEE algorithm is summarised in Algorithm 1.

Remark 3: When $\gamma = 0$, the proposed QKGMEE algorithm translates into KGMEE algorithm [28]. It can be observed that the KGMEE algorithm is a special form of the QKGMEE algorithm, and the QKGMEE algorithm has a much smaller computational burden.

It is obvious to infer that the QKGMEE algorithm will translate into a special algorithm with a QMEE cost function, and the derived algorithm is known to us as QKRMEE. The QKRMEE algorithm and the QKGMEE algorithm share a similar comprehensive derivation procedure. The QKRMEE derivation method is skipped to cut down on repetition, while Algorithm 2 provides an overview of its pseudo-code.

Remark 4: The QKGMEE algorithm translates into the proposed QKRMEE algorithm for $\alpha = 2$. When $\alpha = 2$ and $\gamma = 0$, the proposed QKGMEE algorithm translates into the KRMEE algorithm.

Algorithm 1: QKRMEE

Input: sample sequences $\{d_n, \mathbf{u}_n\}, n = 1, 2, \dots$
Output: function $f(\cdot)$

- 1 **Parameters setting:** select the proper parameters including $\gamma, \alpha,$ and β ;
- 2 **Initialization:** $\mathbf{Q}_1 = [\beta^\alpha \vartheta_2 + \kappa(\mathbf{u}_1, \mathbf{u}_1)]^{-1}$,
 $\mathbf{A}_1 = \mathbf{Q}_1 d_1$;
- 3 **while** $\{d_n, \mathbf{u}_n\} \neq \emptyset$ **do**
- 4 Compute $\mathbf{h}_L, y_L,$ and e_L by

$$\begin{cases} \mathbf{h}_L = \\ [\kappa(u_{n+L-1}, u_n), \dots, \kappa(u_{n+L-1}, u_{n+L-2})]^T, & (30a) \\ y_L = \mathbf{h}_L^T \mathbf{A}_{L-1}, & (30b) \\ e_L = d_L - y_L; & (30c) \end{cases}$$
- 5 Compute $\mathbf{z}_L, \theta_L, \mathbf{r}_L$;
- 6 Update \mathbf{Q}_L and \mathbf{A}_L ;
- 7 **end**

IV. PERFORMANCE ANALYSIS

A. Mean error behavior

By using the QGMEE criterion, the output of the nonlinear system's desired result is

$$d_n = (\mathbf{w}^o)^T \boldsymbol{\varphi}_n + v_n, \quad (35)$$

where \mathbf{w}^o represents the unknown parameter and v_n denotes the zero-mean measurement noise. The weight \mathbf{w} can also, from [32], be expressed as

$$\mathbf{w}_n = \mathbf{w}_{n-1} + (\boldsymbol{\varphi}_n - \boldsymbol{\Phi}_{n-1} \mathbf{z}_n) \mathbf{r}_n^{-1} e_n. \quad (36)$$

Suppose that the weight error definition is

$$\boldsymbol{\varepsilon}_n = \mathbf{w}^o - \mathbf{w}_n, \quad (37)$$

where $\boldsymbol{\varepsilon}_n$ is a vector $\boldsymbol{\varepsilon}_n = [\varepsilon_{1;n} \ \varepsilon_{2;n} \ \dots \ \varepsilon_{m;n}]^T$. Substituting (36) into (37), and we can obtain

$$\boldsymbol{\varepsilon}_n = \mathbf{w}^o - \mathbf{w}_n = \boldsymbol{\varepsilon}_{n-1} - (\boldsymbol{\varphi}_n - \boldsymbol{\Phi}_{n-1} \mathbf{z}_n) \mathbf{r}_n^{-1} e_n. \quad (38)$$

According to (35), one can obtain

$$e_n = \boldsymbol{\varphi}_n^T \mathbf{w}^o + v_n - \boldsymbol{\varphi}_n^T \mathbf{w}_{n-1} \quad (39)$$

Substituting (39) into (38), and we can get

$$\boldsymbol{\varepsilon}_n = (\mathbf{I} - \boldsymbol{\alpha}_n \boldsymbol{\varphi}_n^T) \boldsymbol{\varepsilon}_{n-1} - \boldsymbol{\alpha}_n v_n, \quad (40)$$

where $\boldsymbol{\alpha}_n = (\boldsymbol{\varphi}_n - \boldsymbol{\Phi}_{n-1} \mathbf{z}_n) \mathbf{r}_n^{-1}$. Given that v_n 's mean value is zero, the expectation of $\boldsymbol{\varepsilon}_n$ can be written as

$$E[\boldsymbol{\varepsilon}_n] = (\mathbf{I} - E[\boldsymbol{\alpha}_n \boldsymbol{\varphi}_n^T]) E[\boldsymbol{\varepsilon}_{n-1}]. \quad (41)$$

The eigenvalue decomposition of $E[\boldsymbol{\alpha}_n \boldsymbol{\varphi}_n^T]$ is $E[\boldsymbol{\alpha}_n \boldsymbol{\varphi}_n^T] = \mathbf{K} \boldsymbol{\Omega} \mathbf{K}^T$. \mathbf{K} denotes a square matrix composed of eigenvectors whose diagonal elements are eigenvalues. When we set $\boldsymbol{\varepsilon} = \mathbf{K}^T \boldsymbol{\varepsilon}$, (41) can be further written as

$$E[\boldsymbol{\varepsilon}_n] = (\mathbf{I} - \boldsymbol{\Omega}) E[\boldsymbol{\varepsilon}_{n-1}]. \quad (42)$$

As a result, \mathbf{W} 's maximum eigenvalue $E[\boldsymbol{\alpha}_n \boldsymbol{\varphi}_n^T]$ is less than one, which implies that $E[\boldsymbol{\varepsilon}_n]$ will eventually converge.

Algorithm 2: QKRMEE

Input: sample sequences $\{d_n, \mathbf{u}_n\}, n = 1, 2, \dots$
Output: function $f(\cdot)$

- 1 **Parameters setting:** select the proper parameters γ and σ ;
- 2 **Initialization:** $\mathbf{Q}_{1:S} = [\gamma^2 \vartheta_{2:S} + \kappa(\mathbf{u}_1, \mathbf{u}_1)]^{-1}$,
 (where $\vartheta_{2:S} = L^2 \vartheta_1$), $\mathbf{A}_{1:S} = \mathbf{Q}_{1:S} d_1$;
- 3 **while** $\{d_n, \mathbf{u}_n\} \neq \emptyset$ **do**
- 4 Compute $\mathbf{h}_L, y_{L:S},$ and $e_{L:S}$ by

$$\begin{cases} \mathbf{h}_L = \\ [\kappa(u_{n+L-1}, u_n), \dots, \kappa(u_{n+L-1}, u_{n+L-2})]^T, & (31a) \\ y_{L:S} = \mathbf{h}_L^T \mathbf{A}_{L-1:S}, & (31b) \\ e_{L:S} = d_L - y_{L:S}; & (31c) \end{cases}$$
- 5 Compute $\mathbf{z}_{L:S}, \theta_{L:S}, \mathbf{r}_{L:S}$ using

$$\begin{cases} \mathbf{z}_{L:S} = \mathbf{Q}_{L-1:S} \mathbf{h}_L = \mathbf{Q}_{L-1:S} \boldsymbol{\Phi}_{L-1}^T \boldsymbol{\varphi}_L, \\ \theta_{L:S} = \sum_{h=1}^H \lambda^{L+h} H_h G_\sigma (e_L - c_h), & (32) \\ \mathbf{r}_{L:S} = \boldsymbol{\varphi}_L^T \boldsymbol{\varphi}_L + \sigma^2 \vartheta_{2:S} \theta_{L:S}^{-1} - \mathbf{z}_{L:S}^T \mathbf{h}_L; \end{cases}$$
- 6 Update $\mathbf{Q}_{L:S}$ and $\mathbf{A}_{L:S}$ using

$$\mathbf{Q}_{L:S} = \begin{bmatrix} \mathbf{Q}_{L-1:S} + \mathbf{z}_{L:S} \mathbf{z}_{L:S}^T \mathbf{r}_{L:S}^{-1} & -\mathbf{z}_{L:S} \mathbf{r}_{L:S}^{-1} \\ -\mathbf{z}_{L:S}^T \mathbf{r}_{L:S}^{-1} & \mathbf{r}_{L:S}^{-1} \end{bmatrix}, \quad (33)$$
- 7 and

$$\mathbf{A}_{L:S} = \begin{bmatrix} \mathbf{A}_{L-1:S} - \mathbf{z}_{L:S} \mathbf{r}_{L:S}^{-1} (d_L - c_h) \\ \mathbf{r}_{L:S}^{-1} (d_L - c_h) \end{bmatrix}; \quad (34)$$
- 8 **end**

B. Mean square error behavior

As the noise v_n is never correlated with the $\boldsymbol{\varepsilon}_{n-1}$, the covariance matrix of

$$E[\boldsymbol{\varepsilon}_n \boldsymbol{\varepsilon}_n^T] = \boldsymbol{\alpha}_n E[v_n v_n] \boldsymbol{\alpha}_n^T + (\mathbf{I} - \boldsymbol{\alpha}_n \boldsymbol{\varphi}_n^T) E[\boldsymbol{\varepsilon}_{n-1} \boldsymbol{\varepsilon}_{n-1}^T] (\mathbf{I} - \boldsymbol{\alpha}_n \boldsymbol{\varphi}_n^T)^T. \quad (43)$$

(43) can be abbreviated as

$$\mathbf{T}_n = \mathbf{R}_n \mathbf{T}_{n-1} \mathbf{R}_n^T + \boldsymbol{\Xi}_n \quad (44)$$

with

$$\begin{cases} \mathbf{T}_n = E[\boldsymbol{\varepsilon}_n \boldsymbol{\varepsilon}_n^T], \\ \mathbf{R}_n = (\mathbf{I} - \boldsymbol{\alpha}_n \boldsymbol{\varphi}_n^T), \\ \boldsymbol{\Xi}_n = \boldsymbol{\alpha}_n E[v_n v_n] \boldsymbol{\alpha}_n^T. \end{cases} \quad (45)$$

Given that, $\boldsymbol{\alpha}_n \boldsymbol{\varphi}_n^T$ and $\boldsymbol{\alpha}_n$ are variables that are independent of time [27], one can summarize

$$\begin{cases} \lim_{n \rightarrow \infty} \mathbf{T}_n = \mathbf{T}, \\ \lim_{n \rightarrow \infty} \mathbf{R}_n = \mathbf{R}, \\ \lim_{n \rightarrow \infty} \boldsymbol{\Xi}_n = \boldsymbol{\Xi}. \end{cases} \quad (46)$$

As a result, when $n \rightarrow \infty$, (44) can be written as a real discrete-time Lyapunov equation with the following formula:

$$\mathbf{T} = \mathbf{RTR}^T + \mathbf{\Xi}. \quad (47)$$

From the matrix-vector operator:

$$\begin{cases} \text{vec}(\mathbf{SUV}) = (\mathbf{V}^T \otimes \mathbf{S}) \text{vec}(\mathbf{U}), \\ \text{vec}(\mathbf{S} + \mathbf{V}) = \text{vec}(\mathbf{S}) + \text{vec}(\mathbf{V}), \end{cases} \quad (48)$$

where \otimes represents the Kronecker product and $\text{vec}(\cdot)$ stands for vectorization operation. The closed-form solution of (47) can be written as

$$\text{vec}(\mathbf{T}) = (\mathbf{I} - \mathbf{R} \otimes \mathbf{R})^{-1} \text{vec}(\mathbf{\Xi}). \quad (49)$$

C. Computational Complexity

In comparison to the KRMEE and KRGMEE algorithms, the computational complexity of the proposed QKRMEE and QKRGMEE algorithms is examined. By comparing the pseudocode of these algorithms, it can be deduced that the formulas involved in these algorithms have the same form except for the calculation of $\theta_{L,S}$ and θ_L . The method in [33] for assessing the computational burden of each algorithm is used to make it easier to compare the computational complexity of different algorithms. The difference between the KRMEE and QKRMEE algorithms' computational complexity can therefore be stated as

$$\begin{cases} C_{QKRMEE} = C_{com} + C_{\theta;QKRMEE}, \\ C_{KRMEE} = C_{com} + C_{\theta;KRMEE}, \end{cases} \quad (50)$$

where C_{KRMEE} and C_{QKRMEE} are the computational complexity of one cycle of the KRMEE and QKRMEE algorithms; C_{com} represents the computational complexity of formulas of the same form in both algorithms; $C_{\theta;KRMEE}$ and $C_{\theta;QKRMEE}$ are the computational complexity of ϕ_L in (17) [27] and $\theta_{L,S}$ in (32). The difference $C_{d;MEE}$ in computational complexity between the KRMEE and QKRMEE algorithms can be expressed as

$$C_{d;MEE} = C_{\theta;KRMEE} - C_{\theta;QKRMEE}. \quad (51)$$

Similarly, the difference $C_{d;GMEE}$ in computational complexity between the KRGMEE and QKRGMEE algorithms can be expressed as

$$C_{d;GMEE} = C_{\theta;KRGMEE} - C_{\theta;QKRGMEE}, \quad (52)$$

where $C_{\theta;KRGMEE}$ and $C_{\theta;QKRGMEE}$ are the computational complexity of ψ_L in (30g) [28] and θ_L in (23). The computational complexity of $C_{\theta;KRMEE}$, $C_{\theta;QKRMEE}$, $C_{\theta;KRGMEE}$, and $C_{\theta;QKRGMEE}$ is shown in Table I. Based on the estimation scheme of the computational complexity in [33], one can obtain that

$$\begin{cases} C_{d;MEE} \approx 15L - 14 - 16H, \\ C_{d;GMEE} \approx 19L - 18 - 20H. \end{cases} \quad (53)$$

Remark 5: The reduced computational burden after quantization by approximating the strategy in [33], (53) can reflect the contribution of the quantification mechanism to a certain

TABLE I
THE COMPUTATIONAL COMPLEXITY OF KEY COMPONENTS.

| | \times/\div | $+/-$ | Exponentiation |
|----------------------|---------------|----------|----------------|
| $C_{\theta;KRMEE}$ | $8L - 8$ | $3L - 3$ | $4L - 4$ |
| $C_{\theta;QKRMEE}$ | $9H$ | $3H - 1$ | $4H$ |
| $C_{\theta;KRGMEE}$ | $9L - 9$ | $4L - 4$ | $6L - 6$ |
| $C_{\theta;QKRGMEE}$ | $10H$ | $4L - 1$ | $6H$ |

extent, it is not completely accurate. From (53), the quantization approach can successfully lessen the computational burden on the KRMEE and KRGMEE algorithms when L is big and $L \ll H$. It is worth noting that reducing the computational burden will, to some extent, decrease the steady-state error performance of the suggested algorithms. How to choose the quantization threshold to trade off the performance of the algorithm against the computational complexity is discussed in detail in Section V.

V. SIMULATIONS

To demonstrate the effectiveness of the QKRGMEE and QKRMEE algorithms, we present various simulations, and the MSE is regarded as a tool to measure the algorithm performance in terms of steady-state error. Several noise models covered in this paper are presented before these simulations are implemented, such as mixed-Gaussian noise, Gaussian noise, Rayleigh noise, etc.

- 1) The mixed-Gaussian model [34] takes the following form:

$$v \sim \varsigma \mathcal{N}(a_1, \mu_1) + (1 - \varsigma) \mathcal{N}(a_2, \mu_2), 0 \leq \varsigma \leq 1, \quad (54)$$

where $\mathcal{N}(a_1, \mu_1)$ denotes the Gaussian distribution with mean a_1 and variance μ_1 , and ς represents the mixture coefficient of two kinds of Gaussian distribution. The mixed-Gaussian distribution can be abbreviated as $v \sim M(\varsigma, a_1, a_2, \mu_1, \mu_2)$.

- 2) The Rayleigh distribution's probability density function is written as $r(t) = (t/\chi^2) \exp(-t^2/2\chi^2)$. The noise that follows a Rayleigh distribution is shown as $v \sim R(\chi)$.

In this paper, four scenarios are considered, and the distribution of the noise for these four scenarios is $R(3)$, $M(0.95, 0, 0, 0.01, 64)$, $\mathcal{N}(0, 0.01)$, and $0.2R(3) + 0.8M(0.8, 0, 0, 0.01, 64)$, respectively.

A. Mackey–Glass time series prediction

This subpart tests the QKRMEE and QKRGMEE algorithms' performance to learn nonlinearly using the benchmark data set known as Mackey–Glass (MG) chaotic time series. A nonlinear delay differential equation known as the MG equation has the following form:

$$\frac{ds(t)}{dt} = \frac{0.2s(t - \tau)}{1 + s^{10}(t - \tau)} - 0.1s(t). \quad (55)$$

By resolving the MG equation, 1000 noise-added training data and 100 test data are produced.

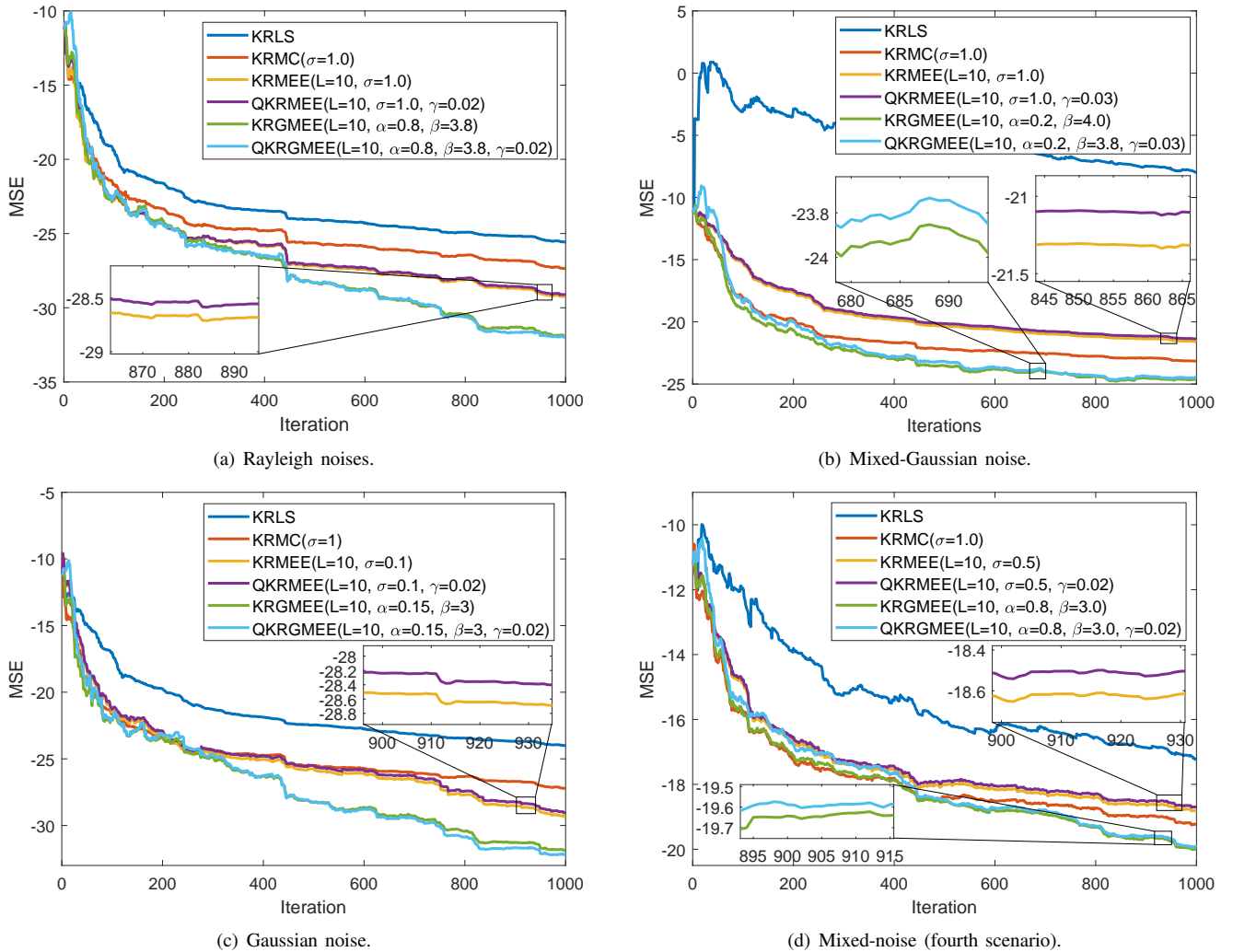


Fig. 1. Convergence curves under different scenarios

In the four aforementioned instances, the performance of the QKRMEE and QKRGMEE algorithms is compared with that of the KRLS [8], KRMC [35], KRMEE [27], and KRGMEE [28] algorithms. In Fig. 1, the parameters of the algorithms and the MSE convergence curves are displayed, and the regularization factors of KRLS-type adaptive filtering algorithms are all 1. It is evident that the proposed QKRMEE and QKRGMEE algorithms perform marginally worse than the KRMEE and KRGMEE algorithms.

B. The relationship between parameters and performance

In this section, we investigated how the shape parameter α , scale parameter β , length of the Parzen window L , and quantization threshold γ of the QKRGMEE algorithm affected performance on the performance in terms of MSE. Since the QKRMEE algorithm is a special form of the QKRGMEE algorithm, one focuses on the influence of parameters on the performance of the QKRGMEE algorithm. The discussion of how the parameter settings affect the functionality of the QKRGMEE algorithm continues to use the MG chaotic time series. The results reached can also serve as a guide for choosing the QKRGMEE algorithm's parameters.

First, the values of these parameters are shown in Fig. 2(a) as we investigate the impact of parameter L on the functionality of the QKRGMEE algorithm. The parameter L is set to $L = 5, 15, 20, 40, 80$ in this simulation. The simulation results are shown in Fig. 2(a) and Table II, and the distribution of the additive noise is the same as it was in the prior simulation. Fig. 2(a) shows the convergence curves of the QKRGMEE algorithm with different L in the first scenario. Table II presents the steady-state MSE with different L and scenarios. Simulations show that the proposed QKRGMEE algorithms' steady-state error lowers as L increases with the four noise categories listed above. In addition, the improvement in terms of performance is not significant when L is greater than 50, thus, it is possible to balance the performance of the algorithm with the amount of computation when L is less than 50.

Second, the influence of the quantization threshold on the performance of the algorithm is shown in Fig. 2(b) and Table III. Fig. 2(b) presents the convergence curve of the MSE with different γ with the presence of Rayleigh noise, and L is set as $L = 50$. Table III shows the MSE, the running time of each iteration, and the number of elements H in the quantized error set with the different γ and scenarios.

TABLE II
THE STEADY-STATE MSE OF THE QKRMEE ALGORITHM WITH DIFFERENT L .

| | $L = 5$ | $L = 10$ | $L = 15$ | $L = 20$ | $L = 30$ | $L = 50$ | $L = 80$ | $L = 100$ |
|----------------|---------|----------|----------|----------|----------|----------|----------|-----------|
| Rayleigh | -32.09 | -32.79 | -33.03 | -33.21 | -33.39 | -34.59 | -35.08 | -35.12 |
| Mixed-Gaussian | -20.30 | -24.46 | -24.43 | -24.94 | -25.13 | -25.63 | -26.13 | -26.23 |
| Gaussian | -29.99 | -30.52 | -30.98 | -31.08 | -31.30 | -31.41 | -31.85 | -31.98 |
| Mixed-noise | -19.36 | -21.13 | -21.32 | -21.42 | -21.44 | -21.45 | -21.65 | -21.69 |

TABLE III
THE STEADY-STATE MSE OF THE QKRMEE ALGORITHM WITH DIFFERENT γ .

| | Rayleigh | | | mixed-Gaussian | | | Gaussian | | | mixed-noise | | |
|---------------------------|----------|---------|-------|----------------|---------|-------|----------|---------|-------|-------------|---------|-------|
| | MSE | Time | H | MSE | Time | H | MSE | Time | H | MSE | Time | H |
| KRLS | -25.35 | 0.00848 | N/A | -7.24 | 0.00848 | N/A | -25.17 | 8.63 | N/A | -16.43 | 0.00872 | N/A |
| KRMEE | -29.65 | 0.01197 | N/A | -24.19 | 0.01252 | N/A | -30.94 | 0.01292 | N/A | -20.27 | 0.01235 | N/A |
| QKRMEE($\gamma = 0.01$) | -29.50 | 0.01189 | 10.65 | -24.07 | 0.01239 | 10.21 | -30.54 | 0.01259 | 5.59 | -20.12 | 0.01225 | 21.9 |
| QKRMEE($\gamma = 0.04$) | -29.01 | 0.01176 | 4.792 | -23.71 | 0.01226 | 6.48 | -30.50 | 0.01228 | 2.68 | -19.45 | 0.01216 | 10.59 |
| QKRMEE($\gamma = 0.1$) | -28.91 | 0.01170 | 1.866 | -22.86 | 0.01218 | 4.55 | -30.47 | 0.01201 | 1.97 | -19.33 | 0.01213 | 6.26 |
| QKRMEE($\gamma = 0.15$) | -28.69 | 0.01169 | 1.436 | -22.13 | 0.01210 | 4.26 | -30.41 | 0.01196 | 1.579 | -19.11 | 0.01212 | 4.73 |
| QKRMEE($\gamma = 0.4$) | -28.48 | 0.01168 | 1.015 | -21.01 | 0.01203 | 3.92 | -30.22 | 0.01189 | 1.201 | -18.65 | 0.01210 | 2.571 |

TABLE IV
THE STEADY-STATE MSE OF QKRMEE ALGORITHM WITH DIFFERENT α .

| | $\alpha = 0.1$ | $\alpha = 0.4$ | $\alpha = 0.8$ | $\alpha = 1.0$ | $\alpha = 2.0$ | $\alpha = 4.0$ | $\alpha = 8.0$ |
|----------------|----------------|----------------|----------------|----------------|----------------|----------------|----------------|
| Rayleigh | -10.77 | -18.24 | -18.86 | -19.25 | -18.46 | -7.35 | -15.07 |
| Mixed-Gaussian | -11.16 | -24.99 | -24.99 | -24.82 | -20.75 | -8.06 | -0.97 |
| Gaussian | -30.51 | -30.49 | -29.04 | -28.69 | -25.24 | -17.88 | -12.10 |
| Mixed-noise | -10.77 | -18.24 | -18.86 | -19.25 | -18.46 | -7.35 | -0.85 |

TABLE V
THE STEADY-STATE MSE OF THE QKRMEE ALGORITHM WITH DIFFERENT β .

| | $\beta = 0.1$ | $\beta = 0.4$ | $\beta = 2.0$ | $\beta = 4.0$ | $\beta = 8.0$ | $\beta = 15.0$ | $\beta = 30.0$ |
|----------------|---------------|---------------|---------------|---------------|---------------|----------------|----------------|
| Rayleigh | -27.33 | -28.56 | -30.26 | -30.63 | -31.15 | -32.07 | -32.89 |
| Mixed-Gaussian | -23.93 | -24.21 | -24.76 | -25.28 | -25.52 | -25.94 | -26.53 |
| Gaussian | -26.69 | -27.50 | -28.28 | -29.16 | -30.06 | -30.13 | -30.19 |
| Mixed-noise | -17.21 | -17.42 | -17.50 | -17.70 | -17.86 | -17.99 | -18.05 |

These KRLS algorithms are measured using MATLAB 2020a, which works on an i5-8400 and a 2.80GHz CPU. Moreover, the KRLS and KRMEE algorithms are used as benchmarks. From these simulation results, it can be inferred that both the running time and the number H decrease as the quantization threshold increases, while the performance of the algorithm also decreases to some extent; moreover, one can obtain $H \ll L$. The suggested range of quantization thresholds is $0.04 \leq \gamma \leq 0.15$, which strikes a balance between the QKRMEE algorithm's efficiency and computing complexity.

Final, it is also addressed how the parameters α and β affect the QKRMEE algorithm's performance. The simulation results are presented in Fig. 2(c), Fig. 2(d), Fig. 3, Table IV, and Table V. Fig. 2(c) and Fig. 2(d) show, respectively, the convergence curves of the steady-state MSE of the method with varying α and β in the presence of Rayleigh noise. The settings of the parameters are also shown in the corresponding figures. The influence surfaces of α and β on the steady-state MSE under different noise are presented in Fig. 3(a) and Fig. 3(b). Table IV and Table V show the pattern of the algorithm's performance with different α and β in different scenarios. From the simulation results, one can obtain that the proposed algorithm works well for values of alpha or beta in the range $0.1 \leq \alpha \leq 1.5$ or $1 \leq \beta \leq 4$ under the given scenarios.

C. EEG data processing

In this part, we use our proposed QKRMEE and QKRMEE algorithms to handle the real-world EEG data. By putting 64 Ag/AgCl electrodes and the expanded 10-20 system, the EEG data can be obtained from [36]. Moreover, the brain data is captured at a sampling rate of 500 Hz. The settings are presented in Fig. 4(a), and the results are displayed in Fig. 4. Here, we use a segment of the FP1 channel data as the input. Fig. 4(a) displays the convergence curves of QKRMEE and its competitor, and Fig. 4(b) presents the surface of MSE with different α and β .

The mean value of H is 7.25 when $L = 50$ and $r = 0.02$, which shows that the quantizer can significantly reduce the computational burden of the algorithm without any significant degradation in the performance of the algorithm. It can be concluded that the performance of the QKRMEE algorithm is much higher than that of the KRMEE algorithm and is comparable to that of the KRMEE algorithm, even if the QKRMEE algorithm has a lower computational complexity.

VI. CONCLUSION

In this paper, We further refined the properties of the QGMEE criterion. On this basis, this QGMEE criterion was combined with the KRLS algorithm, and two new KRLS-type

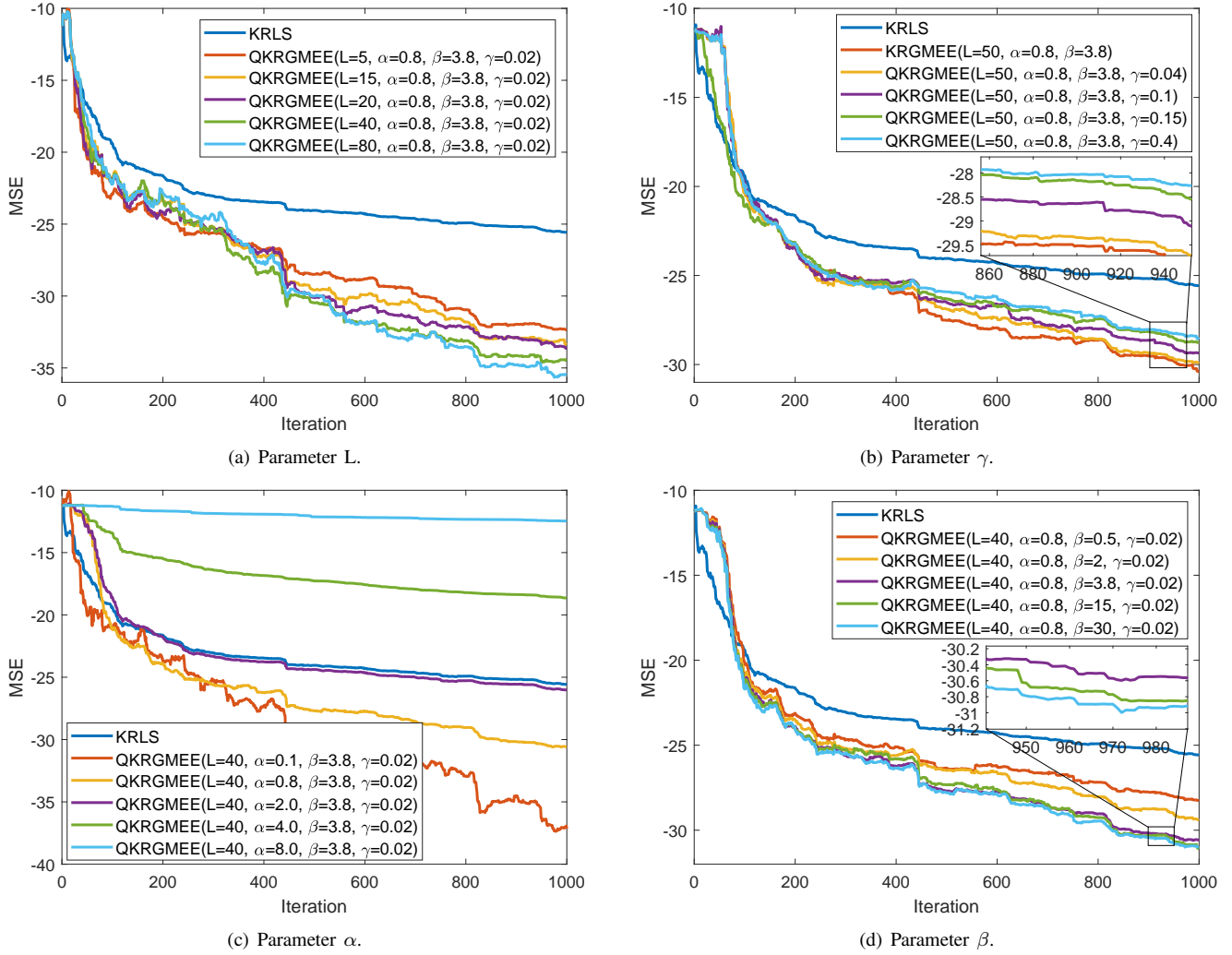


Fig. 2. The performance of the proposed QKRGMEE algorithm with different parameters

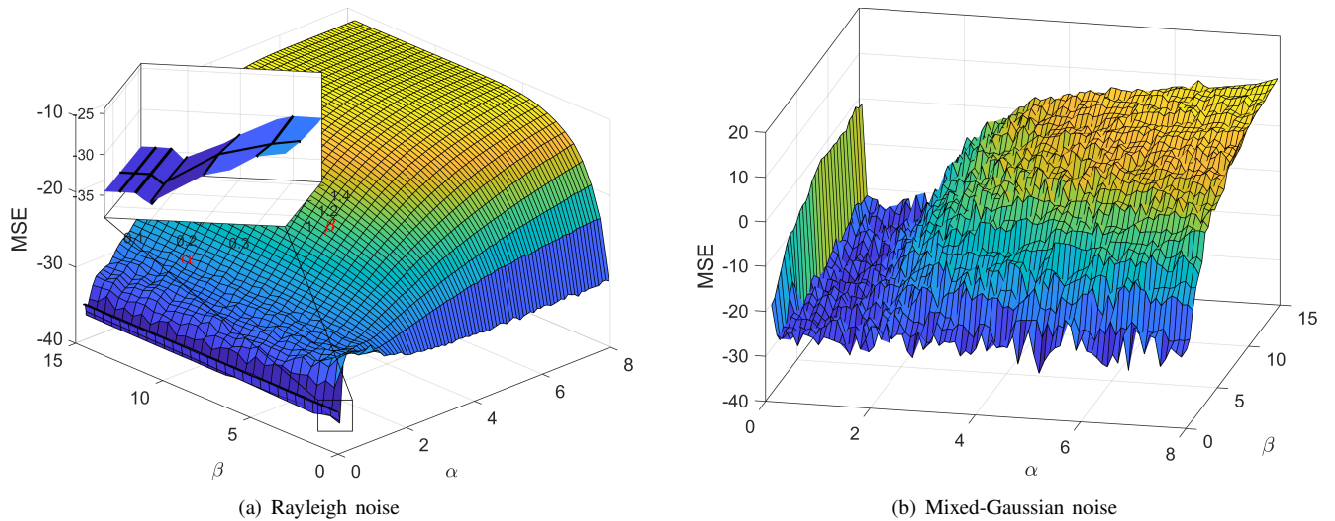
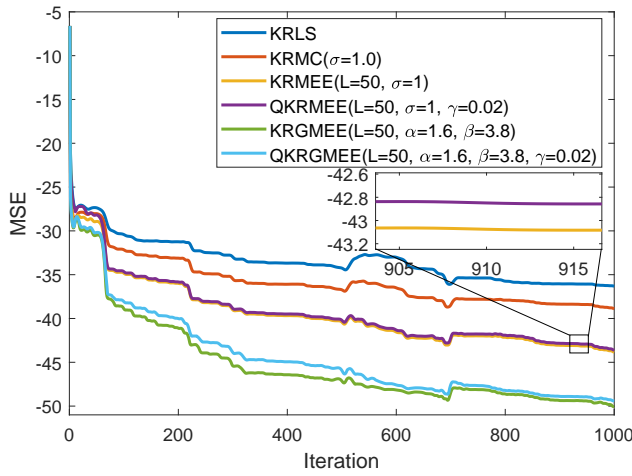
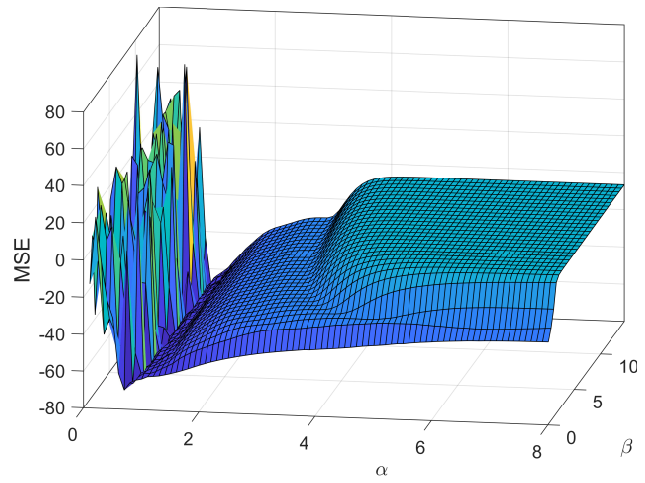


Fig. 3. The performance surfaces of the QKRGMEE algorithm with respect to the parameters α and β in different scenarios



(a) Shape parameter α .



(b) The length of the Parzen's window.

Fig. 4. The performance of the proposed algorithms for processing EEG data.

algorithms were derived, called QKRMEE and QKRGMEE respectively. QKRMEE algorithm is a special case of the QKRGMEE algorithm in which $\alpha = 2$. Moreover, the mean error behavior, mean square error behavior, and computational complexity of the proposed algorithms are studied. In addition, simulation and real experimental data are utilized to verify the feasibility of the proposed algorithms.

VII. ACKNOWLEDGEMENTS

This study was founded by the National Natural Science Foundation of China with Grant 51975107 and Sichuan Science and Technology Major Project No. 2022ZDZX0039, No.2019ZDZX0020, and Sichuan Science and Technology Program No. 2022YFG0343.

REFERENCES

- [1] Lichen Feng, Zunchao Li, Yuanfa Wang, and Chuang Wang. A fast on-chip svm-training system with dual-mode configurable pipelines and msmo scheduler. *IEEE Transactions on Circuits and Systems I: Regular Papers*, 66(11):4230–4241, 2019.
- [2] Kyunghye Kang and Tadashi Shibata. An on-chip-trainable gaussian-kernel analog support vector machine. *IEEE Transactions on Circuits and Systems I: Regular Papers*, 57(7):1513–1524, 2010.
- [3] Jie Chen, Fei Ma, and Jian Chen. A new scheme to learn a kernel in regularization networks. *Neurocomputing*, 74(12):2222–2227, 2011.
- [4] Bernhard Schölkopf, Alexander Smola, and Klaus-Robert Müller. Non-linear component analysis as a kernel eigenvalue problem. *Neural computation*, 10(5):1299–1319, 1998.
- [5] Vinay Chakravarthi Gogineni, Ramesh Sambangi, Daney Alex, Subrahmanyam Mula, and Stefan Werner. Algorithm and architecture design of random fourier features-based kernel adaptive filters. *IEEE Transactions on Circuits and Systems I: Regular Papers*, 70(2):833–845, 2023.
- [6] Badong Chen, Junli Liang, Nanning Zheng, and José C. Principe. Kernel least mean square with adaptive kernel size. *Neurocomputing*, 191:95–106, 2016.
- [7] Weifeng Liu, Puskal P Pokharel, and Jose C Principe. The kernel least-mean-square algorithm. *IEEE Transactions on signal processing*, 56(2):543–554, 2008.
- [8] Yaakov Engel, Shie Mannor, and Ron Meir. The kernel recursive least-squares algorithm. *IEEE Transactions on signal processing*, 52(8):2275–2285, 2004.
- [9] Weifeng Liu, Il Park, Yiwen Wang, and José C. Principe. Extended kernel recursive least squares algorithm. *IEEE Transactions on Signal Processing*, 57(10):3801–3814, 2009.

- [10] Jiacheng He, Gang Wang, Huijun Yu, JunMing Liu, and Bei Peng. Generalized minimum error entropy kalman filter for non-gaussian noise. *ISA Transactions*, 2022.
- [11] Rajib Lochan Das and Manish Narwaria. Lorentzian based adaptive filters for impulsive noise environments. *IEEE Transactions on Circuits and Systems I: Regular Papers*, 64(6):1529–1539, 2017.
- [12] Shiyuan Wang, Lujuan Dang, Badong Chen, Shukai Duan, Lidan Wang, and Chi K. Tse. Random fourier filters under maximum correntropy criterion. *IEEE Transactions on Circuits and Systems I: Regular Papers*, 65(10):3390–3403, 2018.
- [13] Jiacheng He, Gang Wang, Xi Zhang, Hongwei Wang, and Bei Peng. Maximum total generalized correntropy adaptive filtering for parameter estimation. *Signal Processing*, 203:108787, 2023.
- [14] Jiacheng He, Gang Wang, Bei Peng, Qi Sun, Zhenyu Feng, and Kun Zhang. Mixture quantized error entropy for recursive least squares adaptive filtering. *Journal of the Franklin Institute*, 359(3):1362–1381, 2022.
- [15] Weifeng Liu, Il Park, and Jose C Principe. An information theoretic approach of designing sparse kernel adaptive filters. *IEEE transactions on neural networks*, 20(12):1950–1961, 2009.
- [16] Weifeng Liu, Puskal P Pokharel, and Jose C Principe. Correntropy: Properties and applications in non-gaussian signal processing. *IEEE Transactions on signal processing*, 55(11):5286–5298, 2007.
- [17] Badong Chen, Lei Xing, Haiquan Zhao, Nanning Zheng, José C Pri, et al. Generalized correntropy for robust adaptive filtering. *IEEE Transactions on Signal Processing*, 64(13):3376–3387, 2016.
- [18] Ji Zhao, J. Andrew Zhang, Hongbin Zhang, and Qiang Li. Generalized correntropy induced metric based total least squares for sparse system identification. *Neurocomputing*, 467:66–72, 2022.
- [19] Jose C. Principe. *Information Theoretic Learning: Renyi's Entropy and Kernel Perspectives*. Springer Publishing Company, Incorporated, 1st edition, 2010.
- [20] Songlin Zhao, Badong Chen, and José C. Principe. Kernel adaptive filtering with maximum correntropy criterion. In *The 2011 International Joint Conference on Neural Networks*, pages 2012–2017, 2011.
- [21] Zongze Wu, Jiahao Shi, Xie Zhang, Wentao Ma, Badong Chen, and IEEE Senior Member. Kernel recursive maximum correntropy. *Signal Processing*, 117:11–16, 2015.
- [22] Shiyuan Wang, Lujuan Dang, Guobing Qian, and Yunxiang Jiang. Kernel recursive maximum correntropy with nyström approximation. *Neurocomputing*, 329:424–432, 2019.
- [23] Yicong He, Fei Wang, Jing Yang, Haijun Rong, and Badong Chen. Kernel adaptive filtering under generalized maximum correntropy criterion. In *2016 International Joint Conference on Neural Networks (IJCNN)*, pages 1738–1745, 2016.
- [24] Ji Zhao and Hongbin Zhang. Kernel recursive generalized maximum correntropy. *IEEE Signal Processing Letters*, 24(12):1832–1836, 2017.
- [25] Badong Chen, Lujuan Dang, Yuantao Gu, Nanning Zheng, and José C Principe. Minimum error entropy kalman filter. *IEEE Transactions on Systems, Man, and Cybernetics: Systems*, 51(9):5819–5829, 2019.

- [26] Badong Chen, Zejian Yuan, Nanning Zheng, and José C. Principe. Kernel minimum error entropy algorithm. *Neurocomputing*, 121:160–169, 2013. Advances in Artificial Neural Networks and Machine Learning.
- [27] Gang Wang, Xinyue Yang, Lei Wu, Zhenting Fu, Xiangjie Ma, Yuanhang He, and Bei Peng. A kernel recursive minimum error entropy adaptive filter. *Signal Processing*, 193:108410, 2022.
- [28] Jiacheng He, Gang Wang, Kui Cao, He Diao, Guotai Wang, and Bei Peng. Generalized minimum error entropy for robust learning. *Pattern Recognition*, 135:109188, 2023.
- [29] Badong Chen, Lei Xing, Nanning Zheng, and Jose C Principe. Quantized minimum error entropy criterion. *IEEE transactions on neural networks and learning systems*, 30(5):1370–1380, 2018.
- [30] Mahesh K Varanasi and Behnaam Aazhang. Parametric generalized Gaussian density estimation. *The Journal of the Acoustical Society of America*, 86(4):1404–1415, 1989.
- [31] A Smola. Support vector machines, regularization, optimization, and beyond. *Learning with Kernels*, 2002.
- [32] Gang Wang, Jingci Qiao, Rui Xue, and Bei Peng. Quaternion kernel recursive least-squares algorithm. *Signal Processing*, 178:107810, 2021.
- [33] Badong Chen, Xi Liu, Haiquan Zhao, and Jose C. Principe. Maximum correntropy kalman filter. *Automatica*, 76:70–77, 2017.
- [34] Xuxiang Fan, Gang Wang, Jiachen Han, and Yinghui Wang. A background-impulse kalman filter with non-gaussian measurement noises. *IEEE Transactions on Systems, Man, and Cybernetics: Systems*, 53(4):2434–2443, 2023.
- [35] Zongze Wu, Jiahao Shi, Xie Zhang, Wentao Ma, and Badong Chen. Kernel recursive maximum correntropy. *Signal Processing*, 117:11–16, 2015.
- [36] Yajing Si, Xi Wu, Fali Li, Luyan Zhang, Keyi Duan, Peiyang Li, Limeng Song, Yuanling Jiang, Tao Zhang, Yangsong Zhang, et al. Different decision-making responses occupy different brain networks for information processing: a study based on eeg and tms. *Cerebral Cortex*, 29(10):4119–4129, 2019.



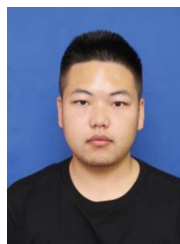
Jiacheng He received the B.S. degree in mechanical engineering from University of Electronic Science and Technology of China, Chengdu, China, in 2020. He is currently pursuing a Ph.D. degree in the School of Mechanical and Electrical Engineering, University of Electronic Science and Technology of China, Chengdu, China. His current research interests include information-theoretic learning, signal processing, and adaptive filtering.



Gang Wang received the B.E. degree in Communication Engineering and the Ph.D. degree in Biomedical Engineering from University of Electronic Science and Technology of China, Chengdu, China, in 1999 and 2008, respectively. In 2009, he joined the School of Information and Communication Engineering, University of Electronic Science and Technology of China, China, where he is currently an Associate Professor. His current research interests include signal processing and intelligent systems.



Kun Zhang received the B.S. degree in electronic and information engineering from Hainan University, Haikou, China, in 2018. He is currently working toward the Ph.D. degree in mechanical engineering with the Mechanical Engineering of the University of Electronic Science and Technology of China, Chengdu, China. His research interests include intelligent manufacturing systems, robotics, and its applications.



Shan Zhong received the B.E. degree in electrical engineering and automation with University of Technology, Chengdu, China in 2020. He is currently pursuing the M.S. degree in B.E. degree in communication engineering with School of Information and Communication Engineering, University of Electronic Science and Technology of China, Chengdu, China. His current research interests include signal processing and target tracking.



His research interests mainly include intelligent manufacturing systems, robotics, and its applications.

Bei Peng received the B.S. degree in mechanical engineering from Beihang University, Beijing, China, in 1999, and the M.S. and Ph.D. degrees in mechanical engineering from Northwestern University, Evanston, IL, USA, in 2003 and 2008, respectively. He is currently a Full Professor of Mechanical Engineering with the University of Electronic Science and Technology of China, Chengdu, China. He holds 30 authorized patents. He has served as a PI or a CoPI for more than ten research projects, including the National Science Foundation of China.



Technology Invention Award.

Min Li obtained a doctoral degree in Mechanical Engineering from Chongqing University, Chongqing, China, in 2012. He is currently an assistant professor in the School of Mechanical Engineering with Southwest Jiaotong University, China. In recent years, he has presided over one major research and development project of the Sichuan Provincial Department of Science and Technology, one Chunhui Program of the Ministry of Education, and four horizontal projects for enterprises. He has won one first prize of the Ministry of Education

